

Characterization of upper limb movement-related EEG dynamics through fractional integrated autoregressive modeling

Laura Cavaliere^{1*}, Vincenzo Catrambone^{1*}, Matteo Bianchi¹, Ana Paula Rocha², and Gaetano Valenza¹

Abstract—The analysis of electroencephalographic (EEG) series associated with movement performance is important for understanding the cortical neural control on motor tasks. While the existence of long-range correlations in physiological dynamics has been reported in previous studies, such a characterization in EEG series gathered during upper-limb movements has not been performed yet. To this end, here we report on a fractional integrated autoregressive analysis of EEG series during different functional classes of motor actions and resting phase, and data were gathered from 33 healthy volunteers. Results show significant differences in EEG long-range correlations on EEG series from characteristic topography.

I. INTRODUCTION

Understanding the neural mechanisms underlying motor control is a pivotal topic in science, with an impact on several fields such as neuroscience, robotics, engineering, and rehabilitation. Particular attention has been devoted to the study of motor control of the hand. This is because the hand is the main tool through which humans interact with the external environment. Studies have also been focused on the upper limb because it guides and optimizes the hand position and orientation with respect to the external targets [1]. The scientific literature on motor control and the associated deficits (e.g., limb apraxia [2]) highlighted that, from a cognitive viewpoint, upper limb movements can be classified into three main categories based on the type of interaction with objects: (i) intransitive movements, movements excluding the use of an object; (ii) transitive actions, movements involving the use of a single object; and (iii) tool-mediated tasks, movements involving the use of an object as a tool to interact with another object [2], [3]. The static functional activity of the three classes has been studied, and significant differences have been found, both through functional magnetic resonance imaging [4] and electroencephalography (EEG) analysis [5], [6].

Among the several neuroimaging techniques employed in the study of brain activity during motor control processes, EEG yields the highest temporal resolution, which allows for an in-depth investigation of brain dynamics. EEG analysis

can be performed through the parametric and non-parametric approaches. The former approach, which does not encounter spectral losses and provides satisfactory frequency resolution, is based on the use of stochastic linear models. Most often, it is based on the autoregressive model (AR) [7]. Classical AR models are well suited for studying short-memory processes, meaning processes with an autocorrelation function (ACF) that decreases exponentially to zero [8]. This behavior implies that observations far apart in time from one another are weakly dependent [8], [9]. Conversely, time-series functions characterized by strong long-range correlation, decaying at a much slower hyperbolic rate, are denoted as long-memory processes.

Sample ACFs derived from EEG time-series functions generally demonstrate a slow decay in ACF coefficients, indicating a non-negligible dependence between observations distant from each other. This suggests the existence of long-range correlations in EEG dynamics, particularly during emotional and musical stimulation [10]. One possible approach to long-memory process description in EEG data is to use fractionally integrated autoregressive (ARFI) models. These models, introduced by *Hosking* in [11], are of special interest because of their capacity to model time-series behavior both in the short- and long-term ranges.

Indeed, *ARFI* models are useful for analyzing several time-series and can also be utilized in the physiological domain [12]. In particular, *ARFI*-moving average (*ARFIMA*) models, which are an extension of the well-known autoregressive moving average (*ARMA*) models, have been used to extract long-memory components from heart rate variability (HRV) recordings. The long-memory component might be individuated by the spectral density function, which follows a $1/f$ power law at very low frequencies [8], [13]. To the best of our knowledge, the characterization of long-memory components and long-range correlation on EEG time-series during motor control tasks has not yet been attempted.

In light of the above, we present a preliminary study aiming to investigate how the brain dynamics of long-memory properties change across the scalp during different upper limb movements. For the first time, the *ARFI* model is applied to EEG-derived power time courses, and the manner in which the EEG dynamics differentiate among different types of upper limb movements is investigated.

II. MATERIALS AND METHODS

A. Experimental dataset

33 right-handed healthy subjects (26 yo on average, 16 females) volunteered to participate in the study. Experiments

¹ Department of Information Engineering & Bioengineering and Robotics Research Center E. Piaggio, School of Engineering, University of Pisa, Italy.

² Faculdade de Ciências & CMUP, Universidade do Porto, Portugal.

* These authors contributed equally to this work.

This research received partial funding from the Italian Ministry of Education and Research (MIUR) in the framework of CrossLab project, and from PRIN2017 project TRAINED 2017L2RLZ2002. A.P. Rocha was partially supported by CMUP, which is financed by national funds through FCT - Fundação para a Ciência e Tecnologia, I.P., project IUDB/00144/2020.

Correspondence to: vincenzo.catrambone@ing.unipi.it

began with an initial baseline acquisition constituting the resting phase, with subjects comfortably sitting, and eyes opened. Consequently, an operator explained to the volunteers the task to be performed, mimicking the movements. These tasks involved three main categories of actions: intransitive, i.e., motions not involving any object (e.g., cover the eyes with the palm of the right hand), transitive, i.e., characterized by the interaction with an object (e.g., take a cup and mimic drinking), and tool mediated, i.e., involving the use of a tool to interact with another object (e.g., reach and grasp a key to open a lock). Each category comprises 10 movements, each repeated 3 times, therefore a total of 90 tasks was performed (i.e., 3 classes \times 10 movements \times 3 repetitions each).

Electrical brain activity was recorded through high-density 128 channels Geodesic EEG Systems 300, with sampling frequency of 500 Hz. The experimental procedure was approved by the local ethical committee. The EEG data is part of a broader publicly available multi-modal, multi-center database on arm motion control [14].

B. EEG processing

Signals were preprocessed to remove noise and any type of artifact contamination. The processing was performed following the Harvard Automated Preprocessing Pipeline for EEG (HAPPE) [15]. Briefly, HAPPE involves channel selection to discard the 38 most external channels, band pass filtering (between 1 and 125 Hz), electrical noise removal, bad channel rejection, ICA decomposition, artifact component recognition and rejection, and average re-referencing. A thorough description of the employed dataset and the applied preprocessing procedure, to avoid noise and movement-related artifacts, can be found in [5].

Power spectral density (PSD) was extracted for selected 90 EEG channels and all segments by using the well-known Welch's method with a 1s Hamming window and overlap of 96%, thus resulting in PSD series with a resolution of 0.04s in time and 1 Hz in the frequency domain. Finally, PSD has been filtered in the classical EEG analysis frequency bands: $\delta \in [1 - 4]Hz$, $\theta \in (4 - 8]Hz$, $\alpha \in (8 - 12]Hz$, $\beta \in (12 - 30]Hz$, and $\gamma \in (30 - 45]Hz$. Time windows of movements executions were segmented, thus having PSD time series of 300 samples length on average.

C. ARFI modeling

A stationary process $\{X_{t_n}\}_{n \in \mathbb{Z}}$ is considered having long-range dependencies if a real number $\alpha \in (0, 1)$ and a constant $c_\rho > 0$ exist, such that:

$$\rho(k) \sim c_\rho |k|^{-\alpha}, \quad \text{for } k \rightarrow \infty \quad (1)$$

where $\rho(k)$ indicates the ACF coefficients, defined as: $\rho(k) = \text{cov}(X_{t_n}, X_{t_n+k}) / \text{var}(X_{t_n})$. Eq. 1 can be formulated in the frequency domain as:

$$f(\lambda) \sim c_f |\lambda|^{-\beta}, \quad \text{for } \lambda \rightarrow 0 \quad (2)$$

where $f(\lambda)$ denotes the spectral density of x_{t_n} , $\beta = (1 - \alpha)$ and c_f is a constant term such that $c_f > 0$ [9].

It is worth to introduce the conditional mean $ARFI(p, d)$ model, as a generalization of the well-known $AR(p)$ model, allowing to model the short as well as the long-memory components of the data. In other words, a process x_{t_n} is said to be $ARFI(p, d)$, if it satisfies the following equation:

$$\phi(B)\nabla^d x_{t_n} = \epsilon_{t_n} \quad (3)$$

where $\{\epsilon_{t_n}\}_{n \in \mathbb{Z}}$ is Gaussian white noise $N(0, \sigma_\epsilon^2)$, $\phi(z) = 1 + \sum_{i=1}^p a_i z^i$ is polynomial of order p in the lag operator B , such that $\phi(z) \neq 0$ for $|z| \leq 1$, B is the backward-shift operator defined as $B^k x_{t_n} = x_{t_n-k}$ and ∇^d is the fractional difference operator defined as:

$$\nabla^d = (1 - B)^d = \sum_{j=0}^{\infty} \binom{d}{j} (-B)^j \quad (4)$$

Thus, d is defined as long-memory parameter and quantifies long-range correlations, whereas p , and the parameters in $\phi(B)$ model short-range dependencies in the mean [8], [16]. In the range $-0.5 < d < 0.5$, the α and β parameters of Eq. 1 and Eq. 2 can be defined as a function of d , as $\alpha = 1 - 2d$ and $\beta = 2d$ [9]. For $0 < d < 0.5$ an $ARFI(p, d)$ process has long-memory, for $d = 0$ $ARFI(p, 0)$ reduces to the usual short-memory $AR(p)$ model [8]. Furthermore, a value of $0.5 < d < 1$ depicts non-stationary and mean-reverting process, as it has been found in Heart-Rate Variability time series [13].

An estimate of the actual parameter d , \hat{d} , can be obtained implementing the Local Whittle (LW) estimator [17], and the LW likelihood function [17], that leads to the definition of the following functional $R(d)$:

$$\hat{d} = \arg \min_{d \in \Theta} R(d) \quad (5)$$

where $\Theta = [\Delta_1, \Delta_2]$ is the closed interval of admissible value for d , Δ_1 and Δ_2 are numbers picked such that $0 < \Delta_1 < \Delta_2 < 1$. $R(d)$ is an objective function, defined as [17]:

$$R(d) = \log \left(\frac{1}{m} \sum_{j=1}^m \lambda_j^{2d} I_{\lambda_j} \right) - \frac{2d}{m} \sum_{j=1}^m \log \lambda_j \quad (6)$$

where $I_{\lambda_j} = \frac{1}{n} \left| \sum_{t=1}^n x_t e^{-it\lambda_j} \right|^2$, with $\lambda_j = \frac{2\pi j}{n}$ for $j = 1, \dots, m$ are the first m harmonics of the periodogram.

In this study, the d -parameter has been estimated on the whole set of 90 EEG channels, 5 PSD bands time series, and for all experimental classes (i.e., rest, intransitive, transitive and tool mediated). The PSD time series were sampled at 25Hz, with an average length of 14 seconds resulting in 300 samples on average.

D. Statistical analysis

For each EEG channel and frequency band, non-parametric Friedman tests for paired samples were applied to evaluate significant changes in the long-memory component between the four categories of movements, while non-parametric Wilcoxon tests for paired samples were used for pair-wise comparisons. For each subject, the extracted d -values were averaged across movements belonging to the

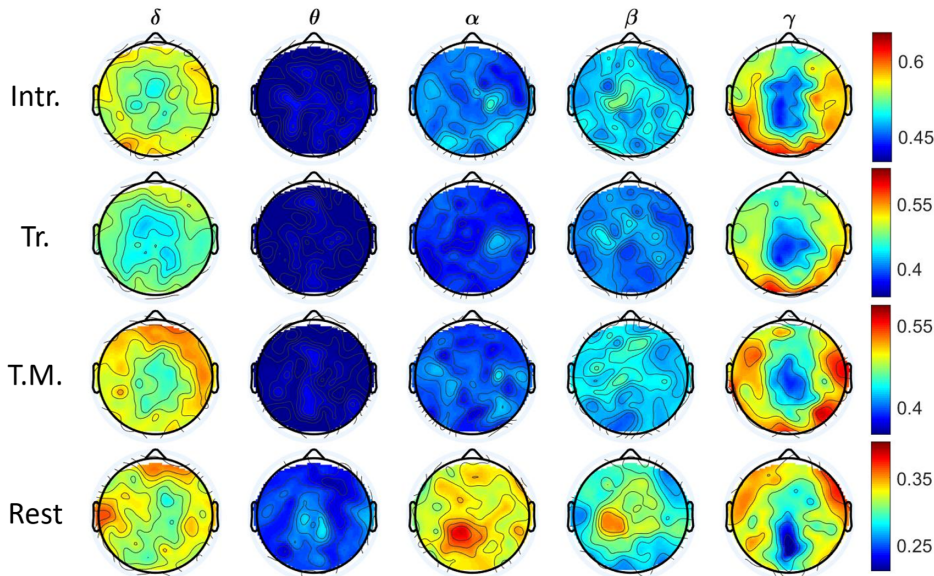


Fig. 1: Topographical representation of the long-term d -value averaged across subjects and tasks.

same class for an effective estimation of class-specific long-term memory parameter. Statistical significance was set to 95%, and p-values were corrected for multiple comparisons through a Bonferroni correction.

III. EXPERIMENTAL RESULTS

Topographical representation of long-memory components: In Figure 1, the topographical representation of the measured d -values as the median across subjects, is depicted. A substantial difference among the five frequency bands is highlighted in all four experimental classes (that is, rest, intransitive *Intr.*, transitive *Tr.*, tool-mediated *T.M.*). Specifically, the θ band always presents the lowest values in the intra-class graphical comparison, and it is followed, in order, by the α and then the β band for the three motion classes (i.e., *Intr.*, *Tr.*, and *T.M.*). In this case, the first difference occurs with the rest category, in which the α band has a visibly higher long-memory parameter d with respect to the β band. The d -values peripheral on the scalp seem to be the highest in all bands, whereas generally homogeneous mid values are depicted in the δ band in all classes. Notably, the four experimental groups have different ranges, with the resting state having the lowest d -values; the other three classes share similar d -value ranges, while the intransitive class achieves a slightly higher range.

Moreover, the spatial distribution of the γ band seems to have a general radial gradient, with lower values in the central regions and higher values in the peripheral regions. In fact, the highest d -values in the γ bands (which are the highest among bands for each class) were measured in the occipital region for intransitive and transitive movements in the right lateral temporal and dorso-parietal electrodes for tool-mediated actions, whereas this is achieved in the prefrontal right lobe in the resting state.

Notably, the rest class depicts a dorso-central cluster of electrodes in the left hemisphere, whose values are evidently higher than those of the other electrodes across the scalp in

both the α and β frequency bands.

Statistical analysis: A statistical comparison highlighted several differences as significant, both in group-wise and pair-wise comparisons, and the results are shown in Figure 2. Long-term d -values are statistically significant across the entire scalp in the θ and α bands in the group-wise Friedman statistic results (see Fig. 2.A). A broad region in the posterior part of the scalp is highlighted in the β frequency range, together with a cluster in most frontal electrodes. A remarkable cluster in the left hemisphere showed significant results from the δ band, spreading from the central and parietal lobes; similar results were observed in the right hemisphere in the dorso-parietal region. It should be noted that no significant changes were detected in the γ frequency range.

Considering the post-hoc statistical comparisons shown in Figs. 2.B, a high level of significance is enhanced in the right portion of the panel when the resting state is compared to the three classes of movements. In particular, this is true in the δ and β bands. Of note, the α band is seldom involved in these comparisons. No significant electrodes are found in the transitives *vs.* tool-mediated tasks, whereas few electrodes in the posterior hemisphere are depicted in the intransitives *vs.* tool-mediated comparison. In the top-right section of Fig. 2.B, that is, in the case of the comparison between intransitive and transitive movements, only the γ frequency does not show significant changes, whereas broad differences are highlighted in other ranges. In particular, the θ and α bands are the most involved, followed by the β band in a broad central region, and the δ band in the left-central area.

IV. DISCUSSION AND CONCLUSION

In this preliminary study, aiming to investigate brain dynamics properties associated with long-range components during different upper limb movements, *ARFI* models were applied to the power spectral density (PSD) time series extracted from EEG signals. In addition to the resting state, experimental data were grouped into three categories accord-

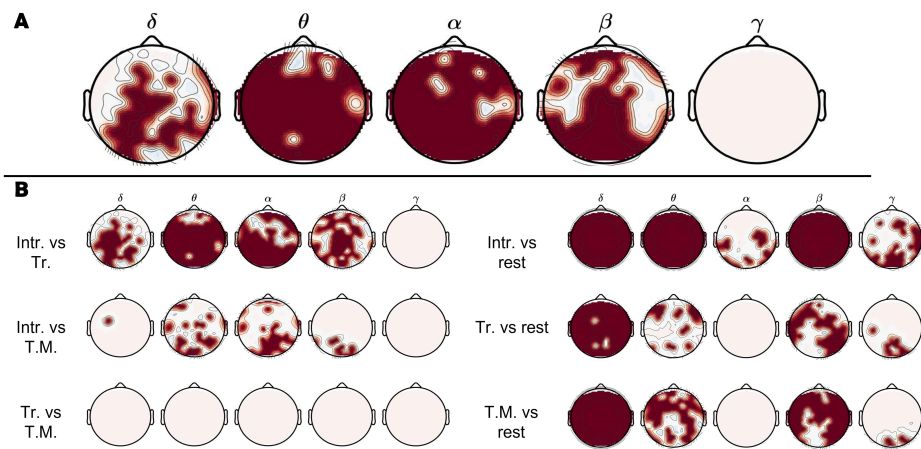


Fig. 2: Bonferroni corrected p-value topographic maps from (A) group-wise Friedman test and (B) pair-wise Wilcoxon test for paired samples, applied to long-memory coefficient d estimates between rest, transitive, intransitive and tool mediated classes. White areas represent not significant regions, whereas red areas represent statistically significant regions.

ing to the type of interaction with objects: intransitives, transitive, and tool-mediated. The main purpose of the present study was to investigate the brain dynamics associated with these tasks and to describe how the long-memory component, previously studied on other physiological signals [8], [13], and quantifiable through the d parameter, affected the EEG dynamics.

Intransitive actions showed higher long-term components with respect to the other two categories of tasks (i.e., transitives and tool-mediated tasks), which display greater similarity to one another. This is in accordance with previous research [4], [5], [18], and might be because the latter involves the use of an object, whereas the former does not. The resting state is strongly different from all the classes of movement, especially in the δ and β frequency ranges. This result suggests that long-term correlations in EEG signals are more affected by the presence of an object rather than by the type of interaction with the object itself, and further studies are needed to investigate these changes.

Regarding power band differences, the d -value distribution extracted in the γ band shows a clear reduction in the d -value over the central cortex region for each class of movement, while brain activity over the tempo-parietal cortices and the occipital cortex was associated with higher d -values. Intriguingly, these results are very similar to those obtained in a previous study on EEG complexity changes across the three categories of movement [6].

To conclude, our results highlighted that the EEG-derived PSD time course has peculiar dynamic properties with different long-term dependencies in motor control tasks. This work represents a preliminary investigation, and future studies are needed to investigate and determine how long-term EEG power dependencies change under different physiological conditions. We propose the long-term dependency parameter as a prospective biomarker of EEG dynamic activity that will prove meaningful in future research.

REFERENCES

[1] C. Prablanc *et al.*, "Neural control of on-line guidance of hand reaching movements," *Progress in brain research*, vol. 142, pp. 155–170, 2003.

[2] A. Bartolo *et al.*, "Cognitive approach to the assessment of limb apraxia," *The Clinical Neuropsychologist*, vol. 22, no. 1, pp. 27–45, 2008.

[3] L. Canzano *et al.*, "The representation of objects in apraxia: From action execution to error awareness," *Frontiers in human neuroscience*, vol. 10, 2016.

[4] G. Handjaras *et al.*, "A topographical organization for action representation in the human brain," *Human brain mapping*, vol. 36, no. 10, pp. 3832–3844, 2015.

[5] V. Catrambone *et al.*, "Predicting object-mediated gestures from brain activity: an eeg study on gender differences," *IEEE Transactions on Neural Systems and Rehabilitation Engineering*, vol. 27, no. 3, pp. 411–418, 2019.

[6] V. Catrambone *et al.*, "Eeg complexity maps to characterise brain dynamics during upper limb motor imagery," in *2018 40th Annual International Conference of the IEEE Engineering in Medicine and Biology Society (EMBC)*, pp. 3060–3063, IEEE, 2018.

[7] L. Sörnmo and P. Laguna, *Bioelectrical signal processing in cardiac and neurological applications*, vol. 8. Academic Press, 2005.

[8] A. Leite *et al.*, "Modelling long-term heart rate variability: an arfima approach," *Biomedizinische Technik*, vol. 51, no. 4, pp. 215–219, 2006.

[9] M. Nielsen and P. Frederiksen, "Finite sample comparison of parametric, semiparametric, and wavelet estimators of fractional integration," *Econometric Reviews*, vol. 24, no. 4, pp. 405–443, 2005.

[10] A. Banerjee *et al.*, "Study on brain dynamics by non linear analysis of music induced eeg signals," *Physica A: Statistical Mechanics and its Applications*, vol. 444, pp. 110–120, 2016.

[11] J. Hosking, "Fractional differencing," *biometrika* 68 165–176," *Mathematical Reviews (MathSciNet): MR614953 Zentralblatt MATH*, vol. 464, 1981.

[12] D. A. Scott and S. J. Schiff, "Predictability of eeg interictal spikes," *Biophysical journal*, vol. 69, no. 5, pp. 1748–1757, 1995.

[13] A. Leite *et al.*, "Beyond long memory in heart rate variability: an approach based on fractionally integrated autoregressive moving average time series models with conditional heteroscedasticity," *Chaos: An Interdisciplinary Journal of Nonlinear Science*, vol. 23, no. 2, p. 023103, 2013.

[14] G. Averta *et al.*, "U-limb: A multi-modal, multi-center database on arm motion control in healthy and post-stroke conditions," *GigaScience*, vol. 10, no. 6, p. giab043, 2021.

[15] L. Gabard-Durnam *et al.*, "The harvard automated processing pipeline for electroencephalography (happe): standardized processing software for developmental and high-artifact data," *Frontiers in neuroscience*, vol. 12, p. 97, 2018.

[16] R. Shumway and D. Stoffer, *Time series analysis and its applications: with R examples*. Springer, 2017.

[17] P. Robinson *et al.*, "Gaussian semiparametric estimation of long range dependence," *The Annals of statistics*, vol. 23, no. 5, pp. 1630–1661, 1995.

[18] V. Catrambone *et al.*, "Toward brain-heart computer interfaces: a study on the classification of upper limb movements using multisystem directional estimates," *Journal of Neural Engineering*, 2021.